

Recalculation, Evaluation, and Prediction of Surface Complexation Constants for Metal Adsorption on Iron and Manganese Oxides

R. W. Smith*[†] and E. A. Jenne

Pacific Northwest Laboratory, Richland, Washington 99352

■ The triple-layer model of the oxide/water interface can be used to calculate the partitioning of metals among solid and aqueous phases. The defensible use of the triple-layer model in groundwater/sediment systems requires an adequate and consistent set of intrinsic adsorption constants. In the present study, published values of p^*K^{int} for cation adsorption on iron and manganese oxides have been used to calculate values for surface complexation constants ($\log K^{SC}$) via

$$\log K_{M(OH)_n}^{SC} = pK_{a2}^{int} - p^*K_{M(OH)_n}^{int} - \log \beta_{1n}$$

where pK_{a2}^{int} is the intrinsic acidity constant and β_{1n} is the n th cation hydrolysis constant. This transformation reduced the variation between $\log K^{SC}$ values determined by different investigators. Uncertainties in acidity constants and variations in site loading with adsorbing metal are the major sources of variation in the values of p^*K^{int} . In addition, ionic strength can affect the values of p^*K^{int} for strongly adsorbed cations. Predictive equations based on ion size and hydrolysis behavior have been derived and missing values of p^*K^{int} for important pollutant metals predicted. Although these equations do not explicitly account for variations in ionic strength and surface loading, they are useful for predicting values of p^*K^{int} with uncertainties of 0.5-0.8 (α -FeOOH) and 0.4-1.5 log units (δ -MnO₂). Recently published K^{SC} values validate the predictive equation developed for the first and second hydrolysis products of thorium. A data base of p^*K^{int} values is presented in which the variability in pK_{a2}^{int} values are removed and missing values estimated.

Introduction

Land disposal of hazardous metals and metalloids is a significant source of priority pollutants (Ag, As, Ba, Cd, Co, Cr, Cu, Hg, Pb, Sb, Se, Tl, and Zn) for groundwater systems. To mitigate the potential hazards of these priority pollutants, the U.S. Environmental Protection Agency (EPA) is developing sediment quality criteria for metals and metalloids (1, 2). The sediment quality criteria will be used in conjunction with water quality criteria to protect aquatic organisms, the food chain to humans, and drinking water from excessive toxic metal contamination. The EPA is using geochemical models and the equilibrium partitioning approach (2) to calculate the speciation, solubility, and adsorption of metals and metalloids in the development of regulations for the shallow land disposal of solid waste.

The triple-layer model of the oxide/water interface (3) is one computational method by which the partitioning of trace metals between sediments and associated aqueous phase can be numerically evaluated. This model requires the activities of uncomplexed metal species, the model-dependent constants (i.e., values of pK_{a1}^{int} , pK_{a2}^{int} , and p^*K^{int}) for each pollutant, and selected surface properties of the sediment. The equilibrium partitioning approach requires the thermodynamic calculation of metal speciation in groundwater and the calculation of the effects of solids

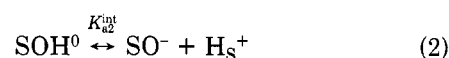
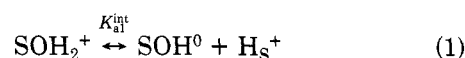
by either adsorption/desorption or dissolution/precipitation mechanisms in limiting the quantity of contaminants available for transport from a disposal site. Computer codes, such as MINTEQA2 (4, 5), that incorporate thermodynamic speciation and solubility calculations and quasi-thermodynamic surface complexation calculations can be used to quantify the activity, hence the bioavailability (6), of pollutants in aqueous systems.

Currently, one fundamental data limitation to using the equilibrium partitioning approach is lack of appropriate adsorption constants for the triple-layer model. This paper provides a set of values for p^*K^{int} for cation adsorption onto iron and manganese oxides and algorithms for predicting p^*K^{int} values. In addition, the major sources of uncertainties in p^*K^{int} are discussed. The results presented complement a related selection of diffuse-layer model constants (7).

Methods

Triple-Layer Model. The conceptual model of surface complexation reactions developed by Yates et al. (8) and modified by Davis et al. (3) partitioned the electric double layer into two constant-capacitance layers and an outer diffuse layer. The oxide surface, containing only protons and hydroxide ions, (the O-plane) is characterized by a charge density, σ_0 , and potential, Ψ_0 . Charged surface sites at the innermost plane lead to specific ion adsorption in the second (β) plane with characteristic charge and potential σ_β and Ψ_β , respectively. In addition, adsorption of the swamping electrolyte occurs in the β -plane.

The acid/base properties of an amphoteric oxide surface are described by two reactions:



where S denotes a structural metal ion of the oxide surface; SOH_2^+ , SOH^0 , and SO^- are the protonated, neutral, and deprotonated surface species, respectively; and surface-plane protons are depicted by H_3^+ . The concentration of protons within the electrical double layer is related to the bulk aqueous proton concentration by the Boltzmann distribution. The resulting mass action expressions for eqs 1 and 2 in terms of aqueous activity of the hydrogen ion become

$$K_{a1}^{int} = \frac{[SOH^0][H^+]}{[SOH_2^+]} \exp\left(\frac{-e\Psi_0}{kT}\right) \quad (3)$$

and

$$K_{a2}^{int} = \frac{[SO^-][H^+]}{[SOH^0]} \exp\left(\frac{-e\Psi_0}{kT}\right) \quad (4)$$

where k is the Boltzmann constant, and T is the temperature in Kelvin. The mass balance on the total number of adsorption sites is imposed via

$$[SOH^0] = SO_{tot} - [SO^-] - [SOH_2^+] \quad (5)$$

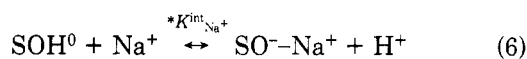
[†] Present address: Idaho National Engineering Laboratory, P.O. Box 1625, Idaho Falls, ID 83415-2107.

Table I. Source of Triple-Layer Model Parameters for Cation Adsorption on Goethite (α -FeOOH), Amorphous Iron(III) Hydrous Oxide, and Manganese Oxide (δ -MnO₂)

α -FeOOH		Am Fe ₂ O ₃ ·nH ₂ O		δ -MnO ₂	
ion	source	ion	source	ion	source
H ⁺	17, 18, 29, 39 ^a -41	H ⁺	9, 41, 43, 44	H ⁺	20, 21
Ca ²⁺	17, 18	Ag ⁺	9	Ca ²⁺	20
Cd ²⁺	19	Ca ²⁺	28, 43	Cu ²⁺	21
Cu ²⁺	19	Cd ²⁺	9, 16, 25	K ⁺	20
Mg ²⁺	17, 18	Co ²⁺	16	Mg ²⁺	20
Pb ²⁺	19	Cu ²⁺	9, 25	Pb ²⁺	21
Pu ⁴⁺	42	Pb ²⁺	9, 25	Zn ²⁺	21
Zn ²⁺	19	Zn ²⁺	9, 16, 25, 43		

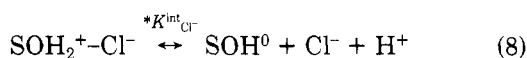
^a As reported in ref 3.

where SO_{tot} is the total number of sites on the solid phase. Similar pairs of expressions can be written for specific adsorption of cations and anions:



$$*K_{\text{Na}^+}^{\text{int}} = \frac{[\text{SO}^- \text{--} \text{Na}^+][\text{H}^+]}{[\text{SOH}^0][\text{Na}^+]} \exp\left(\frac{e\psi_\beta - e\psi_0}{kT}\right) \quad (7)$$

and



$$*K_{\text{Cl}^-}^{\text{int}} = \frac{[\text{SOH}^0][\text{Cl}^-][\text{H}^+]}{[\text{SOH}_2^+ \text{--} \text{Cl}^-]} \exp\left(\frac{e\psi_\beta - e\psi_0}{kT}\right) \quad (9)$$

where SOH₂⁺–Cl[–] represents a protonated surface site (two protons in the O-plane) with a Cl[–] adsorbed in the β -plane, and SO[–]–Na⁺ represents a deprotonated surface site (no protons in the O-plane) with a Na⁺ adsorbed in the β -plane. Detailed derivations of eqs 1–9 are given by Davis and others (3, 9) and reviewed by Leckie (10). The limitations and methodologies in the selection of parameter values for the triple-layer model are discussed by Hayes et al. (11) and Morel and others (12–14).

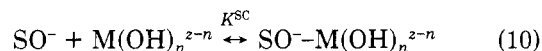
Sources and Evaluation of Uncertainty in Compiled Data. Large differences exist among the values of p^*K^{int} reported by different investigators. Identified sources of these differences include the density and total number of adsorption sites on the oxide surface, the extent of occupancy (loading) of surface adsorption sites, and the formation of inner- and outer-sphere complexes. To evaluate the effects of these sources on the uncertainty of p^*K^{int} values and to select best values, the available values were compiled.

Fifty-six p^*K^{int} values for cation adsorption onto amorphous iron(III) hydrous oxide, α -FeOOH, and δ -MnO₂ were identified in the literature. In addition, 21 $pK_{\text{a}1}^{\text{int}}$ and $pK_{\text{a}2}^{\text{int}}$ values for the above solids were identified. Data have been compiled for amorphous iron(III) hydrous oxide (9, 15, 16), α -FeOOH (17–19), and δ -MnO₂ (20, 21). The sources of these constants, grouped by element, are provided in Table I. Tabulated values for these constants as well as for anions are given by Smith and Jenne (22).

Values of $pK_{\text{a}1}^{\text{int}}$ and $pK_{\text{a}2}^{\text{int}}$ derived from experimental measurements are sensitive to the total number of sites. The site density of an oxide is typically obtained from a surface area measurement of the solid by the BET method (23), and the number of binding sites is determined by tritium exchange, acid/base titration, theoretical calculations, or differential capacitance measurements. These

measurements allow determination of the total number of sites (SO_{tot}, eq 5) per unit mass and per unit surface area of the oxide. By experimental design, [SO[–]] and [SOH₂⁺] are determined directly by potentiometric titration, and [SOH⁰] is calculated from eq 5. Therefore, variations in site density arising from differing experimental methods will be reflected in the values of acidity and complexation constants because of variation in the calculated value of [SOH⁰]. The effects of these variations are illustrated by the two determinations of the surface properties of α -FeOOH by Balistrieri and Murray (17, 18). The site density of 16.8 sites nm^{–2} used in the 1979 paper resulted in values of 4.9 and 10.4 for $pK_{\text{a}1}^{\text{int}}$ and $pK_{\text{a}2}^{\text{int}}$, respectively. The 1981 results, for material prepared under identical conditions and a reported site density of 2.6 sites nm^{–2}, are 5.6 and 9.5 for $pK_{\text{a}1}^{\text{int}}$ and $pK_{\text{a}2}^{\text{int}}$, respectively. The factor of 7 difference between the two reported site densities accounts for the approximate factor of 6 difference between the two sets of acidity constants (18). The actual number of sites per mole of amorphous iron(III) hydrous oxide or δ -manganese(IV) oxide are likely to vary among preparations.

However, it appears that differences between experimental methods to determine site density are a larger source of uncertainty than the actual variations in surface site density. This results in parallel differences occurring in the values of p^*K^{int} for specific ion adsorption because the p^*K^{int} values depend on the values of the acidity constants for the oxide. Davis and Leckie (9) demonstrated that uncertainty in reported p^*K^{int} values can be minimized by writing the reactions in terms of surface-complex formation constants, $\log K^{\text{SC}}$:



$$\log K_{\text{M}(\text{OH})_n}^{\text{SC}} = pK_{\text{a}2}^{\text{int}} - p^*K_{\text{M}(\text{OH})_n}^{\text{int}} - \log \beta_{1n} \quad (11)$$

where β_{1n} is the n th hydrolysis constant for cation M^{z+}. The use of $\log K^{\text{SC}}$, rather than p^*K^{int} , removes the uncertainties associated with site density determinations. This is demonstrated by the data for copper adsorption onto iron(III) hydrous oxides. Values of 4.1 and 8.7 (9) reported for $p^*K_{\text{Cu}}^{\text{int}}$ and $p^*K_{\text{CuOH}}^{\text{int}}$, respectively, compare to values of 3.0 and 7.0 reported by Balistrieri and Murray (19). However, the values of $\log K_{\text{Cu}}^{\text{SC}}$ and $\log K_{\text{CuOH}}^{\text{SC}}$ calculated for these values are 6.6 and 9.9, respectively, for the results of Davis and Leckie (9) and 6.5 and 10.4 for Balistrieri and Murray (19). These results demonstrate that variations in the surface acidity constants arising from uncertainties in site density are a significant source of uncertainty in the values of p^*K^{int} reported in the literature. In addition, these results suggest that values of K^{SC} are not particularly sensitive to the solid polymorph used, as Davis and Leckie (9) used amorphous iron(III) hydrous oxide and Balistrieri and Murray (19) used α -FeOOH.

Uncertainties in the numerical values of p^*K^{int} also arise from differences in the surface loading of the adsorbate on the oxide. Benjamin and Leckie (24) reported that, for most metal ions, fractional adsorption (i.e., moles of metal adsorbed per mole of adsorbate in the system) decreases with increasing total metal concentration in a system with a fixed quantity of adsorbent, even when surface complexation sites are available in excess, resulting in adsorbate concentration dependence of p^*K^{int} . This observation is inconsistent with the implicit assumption made in calculating K^{int} that all surface sites are energetically equivalent. However, Benjamin and others (24, 25) have demonstrated that at very low site coverage the most energetic adsorption site dominates the reaction, so that

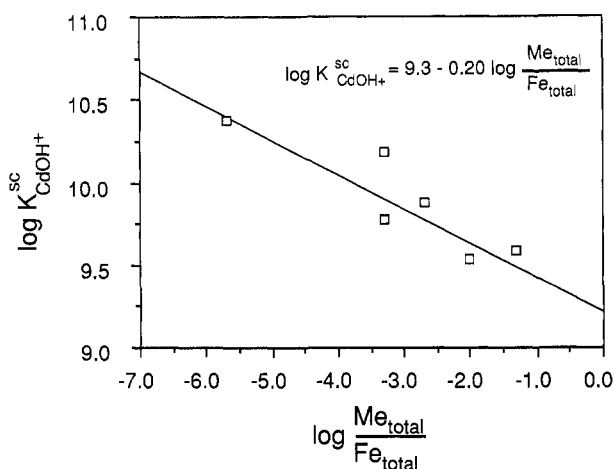


Figure 1. Dependence of $\log K_{\text{CdOH}^+}^{\text{SC}}$ on the experimental adsorbate/adsorbent ratio.

p^*K^{int} is independent of adsorbate concentration. When a sufficient portion of the most energetic sites are filled, the values of p^*K^{int} become dependent on the adsorbate concentration.

Sufficient data are available for Cd^{2+} ($\text{SO}-\text{CdOH}^+$ specifically) to evaluate the consequences of the progressive loading of heterogeneous surface sites on $\log K^{\text{SC}}$ values. Analyses of reported complexation constants indicate that a correlation ($r = 0.89$, significant at the 1% level, Figure 1) exists between $\log K^{\text{SC}}$ and the adsorbate/adsorbent ratio ($\log M_{\text{total}}/\text{Fe}_{\text{total}}$). Figure 1 indicates that for a 10-fold change in the adsorbate/adsorbent ratio, $\log K^{\text{SC}}$ changes by 0.2. However, Van Riemsdijk et al. (26, 27) found that the surface charge-pH curve for metal oxides with some surface site heterogeneity could be adequately described with a homogeneous site adsorption model. Accordingly, Van Riemsdijk et al. (27) were able to model the results of Benjamin and Leckie (24) using a model that assumes homogeneous sites. In addition, some evidence exists that values of p^*K^{int} could be selected that are in reasonable agreement with experiments covering a sizable range of adsorbate/adsorbent ratios (28). However, this may be adsorbate specific. Therefore, it is preferable to evaluate the explicit dependence on loading, as in Figure 1. However, for some protonated anions such as HSeO_4^- and HSO_4^- and unprotonated/unhydrolyzed ions such as Cd^{2+} and CrO_4^{2-} , $\log K^{\text{SC}}$ appears to be independent of the concentrations of the adsorbate and adsorbent (22).

The triple-layer model assumes that all specifically adsorbing ions form outer-sphere complexes and adsorb in the β -plane. However, Hayes and Leckie (29) found no ionic strength dependence of the adsorption of lead and cadmium on α -FeOOH, which they interpreted as indicating that these metals adsorb to the O-plane (i.e., form inner-sphere complexes) rather than in the β -plane. In addition, inner-sphere model calculations for the data of Hayes and Leckie (29) and Cowan et al. (30) indicate that the divalent metal (e.g., Cd^{2+}) is the predominate adsorbing species rather than the hydrolyzed (e.g., CdOH^+) calculated for the outer-sphere model. Furthermore, Hayes et al. (31) demonstrated by X-ray adsorption spectroscopy that selenate forms weakly bonded, outer-sphere complexes and selenite forms strongly bonded, inner-sphere complexes with the surface of α -FeOOH, again suggesting that some ions adsorb to the O-plane. In addition, Cowan et al. (30) found that to model cadmium/alkaline-earth competition experiments with the triple-layer model required the inclusion of both an inner- and outer-sphere complex for cadmium. These results indicate that the complexation

Table II. Surface Complexation Constants ($\log K^{\text{SC}}$) for Cations on Iron(III) Hydrrous Oxide and δ - MnO_2 Substrates

ion	FeOOH		MnO ₂		
	0 ^a	1	0	1	2
Cd ²⁺	5.9	9.7			
Co ²⁺	5.9	8.8			
Cu ²⁺	6.6	10.0	6.1	6.6	6.5
Zn ²⁺	5.9	9.3	4.7	6.4	8.0
Ag ⁺	5.7	10.6			
Pb ²⁺	6.9	11.1	8.0	7.4	
Ca ²⁺	4.3	7.9	0.9		
Mg ²⁺	4.1	6.7	0.3		
Pu ⁴⁺		12.5			

^a Value of n in the reaction $\text{SO}^- + \text{M}(\text{OH})_n^{z-n} = \text{SO}^- - \text{M}(\text{OH})_n^{z-n}$.

of some strongly adsorbed ions is not properly represented by the triple-layer model. To evaluate the effect of ionic strength on values of p^*K^{int} , values of p^*K^{int} for CdOH^+ adsorption as an outer-sphere complex on α -FeOOH were calculated from the experimental results of Hayes and Leckie (29) at ionic strengths of 0.001, 0.001, 0.1, and 1.0 M by using the FITEOL (32) computer code. The values of p^*K^{int} derived showed systematic linear variation with the log of the ionic strength, increasing 0.4 log unit per 10-fold increase in ionic strength. If this result can be generalized, it provides the magnitude of uncertainty that results from using outer-sphere values of p^*K^{int} for calculating adsorption at varying ionic strengths.

Evaluation of Triple-Layer Adsorption Constants

Surface Acidity Constants. The range of $pK_{\text{a1}}^{\text{int}}$ and $pK_{\text{a2}}^{\text{int}}$ values (from sources in Table I) for amorphous iron(III) hydrrous oxide and α -FeOOH exhibit significant overlap. The values of the acidity constants for all iron(III) hydrrous oxides are normally distributed with mean values of 5.0 ± 0.5 and 10.9 ± 0.5 for $pK_{\text{a1}}^{\text{int}}$ and $pK_{\text{a2}}^{\text{int}}$, respectively (22). These results suggest that the effect of crystallinity on the amphoteric behavior of surface oxygen is of secondary importance; the amphoteric behavior is dominated by the characteristics of the Fe(III)-O bond. If this result can be generalized, then acidity constants and values for p^*K^{int} determined for a single oxide polymorph can be used for all polymorphs.

Two sources of surface acidity constants for δ - MnO_2 are reported in Table I. The differences between the values of $pK_{\text{a2}}^{\text{int}}$ for the two oxides are much larger than can be accounted for by the reported differences in site density and may result from the use of materials with differing surface properties. The preparation of δ - MnO_2 with reproducible surface properties is difficult (33). The value of Catts and Langmuir (21) ($pK_{\text{a2}}^{\text{int}} = 4.2$) is selected because the measured values of p^*K^{int} for metals reported here are derived from their study, and because Balistrieri and Murray (20) determined values for only Ca^{2+} , Mg^{2+} , and H^+ .

Swamping Electrolyte p^*K^{int} . Values of $\log K^{\text{SC}}$ for swamping electrolyte ions were calculated from the sources in Table I by use of eq 11. The average values of $\log K^{\text{SC}}$ were combined with the average acidity constants for iron(III) hydrrous oxide to calculate p^*K^{int} values of 9.3 ± 0.5 for Na^+ and K^+ , 7.5 ± 0.3 for NO_3^- , and 6.2 ± 0.6 for Cl^- .

Metal p^*K^{int} . Reported in Table II are mean values of surface complexation constants ($\log K^{\text{SC}}$) for cations calculated by using eq 11, the values of p^*K^{int} and $pK_{\text{a2}}^{\text{int}}$ from the sources reported Tables I, and hydrolysis constants given in Table III (22). Uncertainties in the values of K^{SC} are estimated as ± 0.5 for $\log K_M^{\text{SC}}$ and ± 0.8 for \log

Table III. Values of Hydrolysis Constants (35, 38),^a g_1 , g_2 , and Ionic Radius (r) for Cations (36)

species	$\log \beta_{11}$	$\log \beta_{12}$	g_1	g_2	r
Ag ⁺	-12.0	-24	6	1	0.67
Ba ²⁺	-13.47		4	1	1.36
Ca ²⁺	-12.85		4	1	1.00
Cd ²⁺	-10.08	-20.35	8	2	0.97
Co ²⁺	-9.65	-18.8	8	1	0.74
Cu ²⁺	-7.93	-13.7 ^b	8	1	0.62
Fe ²⁺	-9.5	-20.6	8	1	0.77
Hg ²⁺	-3.4		8	5	0.69
Mg ²⁺	-11.44		4	1	0.72
Mn ²⁺	-10.59	-22.2	8	1	0.82
Pb ²⁺	-7.71	-17.12	16	1	0.94
Pu ⁴⁺	-0.5		12	3	0.93
Tl ⁺	-13.21		12	0	1.50
Zn ²⁺	-8.96	-16.76	8	1	0.74

^a Parallel calculations using hydrolysis constants from the MINTEQ geochemical code (based on ref 45) resulted in slightly different values for $\log K^{sc}$ (Table III). However, the coefficients determined for eq 15 were identical with those determined by using the above constants and reported in the text. In addition, by the nature of the calculations, p^*K^{int} values in Table V for ions listed in Table III are independent of the value of the hydrolysis constant. ^b Reference 46.

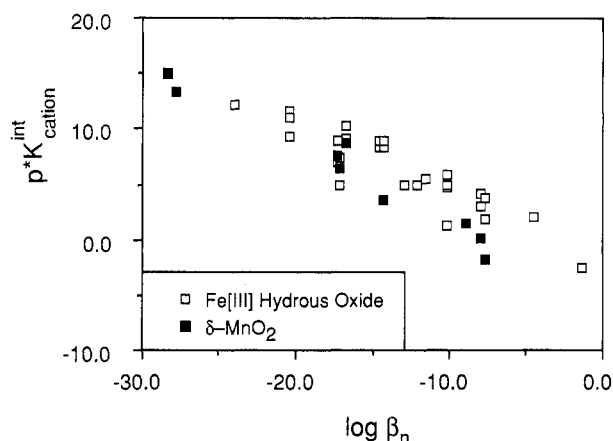


Figure 2. Variation of p^*K^{int} with the hydrolysis constants for cations.

K_{MOH}^{SC} (22). Examination of Table II confirms the Davis and Leckie (9) observation of similarities among values of $\log K^{SC}$, with values of 5.7 ± 1.0 and 9.3 ± 1.4 (excluding Pu^{4+}) for $\log K_M^{SC}$ ($n = 0$) and $\log K_{MOH}^{SC}$ ($n = 1$), respectively.

Prediction of p^*K^{int}

A correlation between the intrinsic stability constants of surface complexes and corresponding values for cation hydrolysis constants has been recognized (e.g., ref 34). Figure 2 displays the relationship between values of p^*K^{int} and values of $-\log \beta_{1n}$ (Table III) for cations. Although general correlations are apparent, the use of such plots to predict values of p^*K^{int} for which measured values are unavailable is of limited use because of the large uncertainties (standard error of 1.2 log units for α -FeOOH) associated with such estimates. Such correlations represent little advantage over using the mean values of 5.7 ± 1.0 and 9.3 ± 1.4 for $\log K_M^{SC}$ and $\log K_{MOH}^{SC}$, respectively, derived from the results for iron(III) hydrous oxides presented in Table II. Because the correlation observed between p^*K^{int} and $\log \beta_{1n}$ is probably a result of the dependency of both equilibrium constants on properties such as charge and size of the aqueous ions, a more reliable approach to estimating p^*K^{int} is to use a method analogous to those developed to estimate hydrolysis constants.

Baes and Messmer (35) derived expressions for estimating first hydrolysis constants for cations from the size-to-charge ratio. They found that the cation β_{11} values were described by four equations with the same slopes and different intercepts. Subsequently, Brown et al. (36) found that, if effective nuclear charge was used instead of simple charge, cation β_{11} values for all cations could be described by a single expression:

$$\log \beta_{11} = \text{intercept} + \text{slope} \left[g_1 \left(\frac{z}{r^2} + g_2 \right) \right] \quad (12)$$

where

$$g_1 = (1 + 2S + D)(z + 2) \quad (13)$$

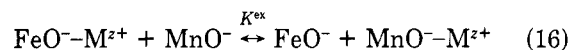
$$g_2 = g(n)(z - 1) + 0.1d(n - 3)^2(1 - S) \quad (14)$$

and where z is the formal charge, r is the ionic radius, S is equal to 0 if there are no s electrons in the outermost shell of the ion and equal to 1 if such electrons are present, D is the number of d electrons in the neutral metal, n is the principal quantum number of the outermost shell of the ion, $g(n)$ is equal to 0 when n is 1 and equal to 1 when n is greater than 1, and d is the number of d electrons in the ion. The significance of the terms in eqs 12–14, as well as the derivations of these equations, is given elsewhere (36). Values of g_1 , g_2 , and r for cations considered in this study are reported in Table III.

An expression of the same general form as eq 12 was fit by means of least squares to values of $\log K^{SC}$ (Table II). The resulting expression is

$$\log K^{SC} = a_0 + 0.10 \left[g_1 \left(\frac{z}{r^2} + g_2 \right) \right] + a_1 \log \beta_{1n} \quad (15)$$

where $\log \beta_{1n}$ is the n th aqueous hydrolysis constant for the surface complex (for SO–M, $n = 0$; SO–MOH, $n = 1$, Table III), and a_0 and a_1 are constants with values of 2.3 and -0.37 ($r = 0.95$, $n \leq 1$), respectively, for iron(III) hydrous oxides and 1.0 and -0.10 ($r = 0.93$, $n \leq 2$) for manganese(IV) oxide. The first two terms on the right side of eq 15 are equivalent to eq 12. The third term allows the prediction of constants for hydrolyzed surface species (i.e., SO–M(OH) _{n} , $n \geq 1$), as $\log \beta_{10}$ is 0 by convention. The value (0.10) of the coefficient of the charge-to-size term in eq 15 was found to be identical for both the Fe(III) and Mn(IV) systems. This means that for a reaction of the type



K^{ex} is independent of the cation considered. If this observation were applied to all oxides, the limited number of p^*K^{int} values for cations on aluminum(III) and titanium(IV) oxides could be used to estimate values of a_0 and a_1 in eq 15 and values of $\log K^{SC}$ could be estimated for number of cations on these other oxides.

Equation 15 is depicted graphically for iron(III) hydrous oxide in Figure 3. Using eq 15 enables relatively accurate prediction of the values of $\log K^{SC}$. Excluding silver, the average differences between calculated and observed values are ± 0.5 for $\log K_M^{SC}$ and ± 0.8 for $\log K_{MOH}^{SC}$ on iron(III) hydrous oxide. For δ -MnO₂ the uncertainties are ± 1.5 for $\log K_M^{SC} \pm 0.4$ for $\log K_{MOH}^{SC}$, and ± 1.2 for $\log K_{MOH_2}^{SC}$. This uncertainty is comparable with the uncertainty in the measured values. Comparison of the uncertainties [0.8 log unit for hydrous iron(III) oxide] associated with eq 15 for surface complexes such as CdOH⁺ with the effect on p^*K^{int} arising from progressive site loading and inner- vs outer-sphere complexes (discussed earlier) indicates that (1) large

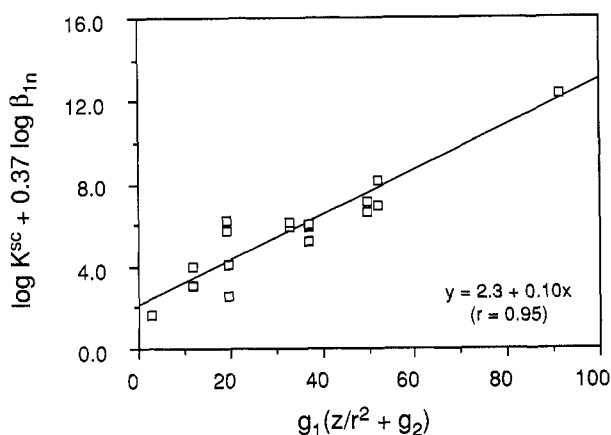


Figure 3. Representation of eq 15 for the prediction of surface complexation constants ($\log K^{\text{sc}}$) for cations on iron(III) hydrous oxides.

Table IV. Comparison of Values of $\log K^{\text{sc}}$ Measured for Thorium (37) and Predicted Independently from eq 15

Th(OH) _n n	FeOOH		MnO ₂	
	H ^a	S ^b	H	S
0	10.5	10.8	nv	
1	12.0	12.0	nv	
2	14.1	13.3	10.6	10.5
3	11.4	15.1	9.9	11.2
4	8.7	16.7	7.7	11.8

^a Reference 37. ^b Equation 15.

variations in the adsorbate-to-adsorbent ratio (approximately a factor of 10 000) are required to shift a p^*K^{int} value by 0.8 log unit, and (2) shifts in ionic strength by a factor of approximately 100 are required to shift a p^*K^{int} value by 0.8 log unit. In practice, this means that given the uncertainties in estimating values of p^*K^{int} with eq 15, progressive surface loading and inner-sphere complexing can be ignored for most groundwater systems. However, it may be that a portion of the uncertainties associated with eq 15 results from the failure to explicitly consider surface heterogeneity and inner-sphere complex formation.

The values of $\log K^{\text{sc}}$ for silver complexes on iron(III) hydrous oxides predicted by eq 15 differ significantly from the measured values of Davis and Leckie (9). The reason for these differences is not clear.

Recent work (37) has defined values of p^*K^{int} for thorium adsorption onto α -FeOOH and δ -MnO₂. As the results of Hunter et al. (37) were published after the development of the regression equations (22), they provide an opportunity to test the validity of eq 15 for predicting triple-layer constants. Values of $\log K^{\text{sc}}$ calculated from the results of Hunter et al. (37) and independently predicted from eq 15 are given in Table IV. As may be seen, the agreement is very good for low values of n . At higher values of n , significant differences between predicted and observed values occur. This is not surprising because eq 15 is based primarily on constants for mono- and divalent cations that do not form surface complexes with values of n larger than 1 or 2. In addition, the hydrolysis behavior of Th⁴⁺ ions is dominated by the formation of polynuclear species (38) and errors in the values of $\log \beta_{1n}$ where $n > 1$ cannot be ruled out. In summary, it appears that eq 15 can be used to predict, with the confidence specified earlier, values of $\log K^{\text{sc}}$ for cations surface complexes with low n values.

Values of p^*K^{int} can be calculated for a large number of ions of interest in groundwater/sediment systems by using eq 11, the values of $\log K^{\text{sc}}$ (Table II), the values of

Table V. Triple-Layer Intrinsic Complexation Constants for Cations on Iron and Manganese Hydrous Oxides Consistent with Values of 10.9 and 4.2 for pK_{a2}^{int} for Iron(III) and Manganese(IV) Oxides, Respectively

cation	Fe(III)		Mn(IV)		
	0 ^a	1	0	1	2
Ag ⁺	5.2	12.3	3.3 ^b	13.6 ^b	
Ba ²⁺	7.8 ^b	16.3 ^b	4.4 ^b		
Ca ²⁺	6.6	15.9	5.3		
Cd ²⁺	5.0	11.3	1.9 ^b	10.6 ^b	19.4 ^b
Co ²⁺	5.0	11.8	1.5 ^b	9.8 ^b	17.6 ^b
Cu ²⁺	4.3	8.8	0.1	7.5	13.4
Fe ²⁺	5.1 ^b	11.1 ^b	1.7 ^b	9.9 ^b	19.4 ^b
Hg ²⁺	1.0 ^b	3.1 ^b	-2.4 ^b	0.5 ^b	
Mg ²⁺	6.8	15.6	5.9		
Mn ²⁺	5.4 ^b	12.1 ^b	2.0 ^b	11.1 ^b	21.1 ^b
Pb ²⁺	4.0	7.5	-1.8	6.5	
Tl ⁺	8.1 ^b	16.4 ^b	4.7 ^b	16.0 ^b	
Zn ²⁺	5.0	10.6	1.5	8.8	15.0

^a Value of n in the reaction $\text{SOH}^0 + \text{M}^{2+} + n\text{H}_2\text{O} = \text{SO}^-\text{M}(\text{OH})_{n-2} + (n+1)\text{H}^+$. ^b Estimated.

$\log \beta_{1n}$ (Table III), and the values of pK_{a2}^{int} given above. For cations not given in Table II, eq 15 can be combined with

$$p^*K^{\text{int}} = pK_{a2}^{\text{int}} - \log K^{\text{sc}} - \log \beta_{1n} \quad (17)$$

and the values for pK_{a2}^{int} given above to yield

$$p^*K^{\text{int}} = 8.6 - 0.63 \log \beta_{1n} - 0.10 \left[g_1 \left(\frac{z}{r^2} + g_2 \right) \right] \quad (18)$$

for cation complexes with iron(III) hydrous oxides and

$$p^*K^{\text{int}} = 5.2 - 0.86 \log \beta_{1n} - 0.10 \left[g_1 \left(\frac{z}{r^2} + g_2 \right) \right] \quad (19)$$

for cation complexes with δ -manganese(IV) oxides. Equations 18 and 19 have been used with values of $\log \beta_{1n}$, g_1 , and g_2 (Table III) to estimate values of p^*K^{int} (Table V) for pollutant cations for which experimentally determined values are not available. Values of p^*K^{int} that are consistent with acidity constants different from those used can be calculated by using eq 17. In addition, values of p^*K^{int} for ions not considered in this study can be estimated from eqs 18 and 19. The use of these estimates will facilitate initial efforts to model the behavior of pollutants and trace metals in groundwater/sediment systems.

A consistent set of outer-sphere p^*K^{int} values for cation adsorption on hydrous iron(III) oxide and δ -MnO₂ is reported in Table V. These values have been recalculated from literature results in an effort to remove the uncertainties associated with site density. All values are consistent with values of 10.9 and 4.2 for pK_{a1}^{int} for hydrous iron(III) oxide and δ -MnO₂, respectively. The values presented are consistent with an ionic strength of 0.1 M; however, given the effect of ionic strength on p^*K^{int} , these values can be used for more dilute groundwaters. The effects of surface site heterogeneity on values of p^*K^{int} have been found to be small compared with other uncertainties and can be ignored. As all values given in Table V are for outer-sphere complexes, the application of the triple-layer model to mixed electrolytes will tend to overpredict the competition effects between inner-sphere complex forming ions (e.g., Cd²⁺ and Pb²⁺) and major electrolyte cations (30).

Conclusions

The most significant source of variation among values of p^*K^{int} reported in the literature is the choice of the values of $p^*K_{a1}^{\text{int}}$ and $p^*K_{a2}^{\text{int}}$ for the adsorbent solid phase. This variation is primarily because of the value of the site

density used, with different techniques giving different values for materials prepared under nearly identical conditions. These variations in p^*K^{int} can be removed by writing the reactions so as to remove the pH dependence. The results presented here demonstrate the need for careful characterization of the number of surface sites and the need for an evaluation of the methods used for such determinations.

Values of p^*K^{int} can be predicted from effective charge, ion size, and hydrolysis behavior of the aqueous ions involved. The use of these predicted values allows an initial evaluation of the importance of adsorption as a mechanism for limiting the aqueous concentration of pollutants for combinations of adsorbates and adsorbents that have not been experimentally evaluated. In addition, such evaluation can be useful in defining systems for which experimental determination would be most beneficial and defining previous experimental studies that may be in error. Furthermore, the variation of K^{SC} with site loading and ionic strength indicates the need to routinely evaluate these variables in future determinations of p^*K^{int} values and in applications of the triple-layer model.

Acknowledgments

We thank D. S. Brown and N. T. Loux for their interest and support, and N. T. Loux, J. P. McKinley, and J. M. Zachara for critical reviews and comment. C. E. Cowan is thanked for assistance in calculating intrinsic constants using the FITEQL computer code.

Registry No. Ag, 7440-22-4; Ba, 7440-39-3; Ca, 7440-70-2; Cd, 7440-43-9; Co, 7440-48-4; Cu, 7440-50-8; Fe, 7439-89-6; Hg, 7439-97-6; Mn, 7439-96-5; Pb, 7439-92-1; Tl, 7440-28-0; Zn, 7440-66-6; MnO₂, 1313-13-9; goethite, 1310-14-1.

Literature Cited

- Jenne, E. A.; DiToro, D. o. M.; Allen, H. E.; Zarba, C. Z. In *Proceedings of the International Conference on Chemicals in the Environment*; Lester, J. N., Perry, R., Sterritt, R. M., Eds.; Selper Ltd.: London, 1986; p 560.
- Shea, D. *Environ. Sci. Technol.* **1988**, *22*, 1256.
- Davis, J. A.; James, R. O.; Leckie, J. O. *J. Colloid Interface Sci.* **1978**, *63*, 480.
- Felmy, A. R.; Girvin, D. C.; Jenne, E. A. *MINTEQA: A Computer Program for Calculating Aqueous Geochemical Equilibria*; (NTIS PB84-157148) EPA-600/3-84-032; National Technical Information Service: Springfield, VA, 1984.
- Brown, D. S.; Allison, J. D. *MINTEQA1, An Equilibrium Metal Speciation Model: User's Manual*; EPA/600/3-87/012; U.S. Environmental Protection Agency: Athens, GA, 1987.
- Cowan, C. E.; Jenne, E. A.; Kinnison, R. R. In *Aquatic Toxicology and Environmental Fate*; Poston, T., Purdy, R., Eds., American Society for Testing and Materials: Philadelphia, PA, 1986; p 463.
- Dzombak, D. A. Ph.D. Dissertation, Massachusetts Institute of Technology, Cambridge, MA, 1986.
- Yates, D. E.; Levine, S.; Healy, T. W. *J. Chem. Soc., Faraday Trans. 1* **1974**, *70*, 1807.
- Davis, J. A.; Leckie, J. O. *J. Colloid Interface Sci.* **1978**, *67*, 90.
- Leckie, J. O. In *Metal Speciation: Theory, Analysis and Application*; Kramer, J. R., Allen, H. E., Eds.; Lewis Publishers, Inc.: Chelsea, MI, 1988; p 41.
- Hayes, K. F.; Redden, G.; Ela, W.; Leckie, J. O. *Application of Surface Complexation Models for Radionuclide Adsorption—Sensitivity Analysis of Model Input Parameters*; NUREG/CR-5547, PNL-7239; U.S. Nuclear Regulatory Commission: Washington, D.C. 1990.
- Morel, F. M. M.; Yeasted, J. G.; Westall, J. G. In *Adsorption of Inorganics at Solid-Liquid Interfaces*; Anderson, M. C., Rubin, A. J., Eds.; Ann Arbor Science: Ann Arbor, MI, 1981; p 263.
- Westall, J. C.; Holh, H. *Adv. Colloid Interface Sci.* **1980**, *12*, 265.
- Westall, J. C. In *Geochemical Processes at Mineral Surfaces*; Davis, J. A., Hayes, K. F., Eds.; ACS Symposium Series 323; American Chemical Society: Washington, DC, 1986; p 54.
- Davis, J. A.; Leckie, J. O. *J. Colloid Interface Sci.* **1980**, *74*, 32.
- Benjamin, M. M.; Bloom, N. S. In *Adsorption from Aqueous Solutions*; Tewari, P. H., Ed.; Plenum: New York, 1981; p 41.
- Balistreri, L. S.; Murray, J. W. In *Chemical Modeling in Aqueous Systems*; Jenne, E. A., Ed.; American Chemical Society: Washington, DC, 1979; p 275.
- Balistreri, L. S.; Murray, J. W. *Am. J. Sci.* **1981**, *281*, 788.
- Balistreri, L. S.; Murray, J. W. *Geochim. Cosmochim. Acta* **1982**, *46*, 1253.
- Balistreri, L. S.; Murray, J. W. *Geochim. Cosmochim. Acta* **1982**, *46*, 1041.
- Catts, J. G.; Langmuir, D. *Appl. Geochem.* **1986**, *1*, 255.
- Smith, R. W.; Jenne, E. A. *Compilation, Evaluation and Prediction of Triple-Layer Model Constants for Ions on Fe(III) and Mn(IV) Hydrrous Oxides*. PNL-6754; Pacific Northwest Laboratory: Richland, WA, 1988.
- Brunauer, S.; Emmett, P. H.; Teller, E. *J. Am. Chem. Soc.* **1938**, *60*, 309.
- Benjamin, M. M.; Leckie, J. O. *J. Colloid Interface Sci.* **1981**, *79*, 209.
- Benjamin, M. M. *Effects of Competing Metals and Complexing Ligands on Trace Metal Adsorption at the Oxide/Solution Interface*; University Microfilms International: Ann Arbor, MI, 1978.
- Van Riemsdijk, W. H.; Bolt, G. H.; Koopal, L. K.; Blaakmeer, J. *J. Colloid Interface Sci.* **1986**, *109*, 219.
- Van Riemsdijk, W. H.; De Wit, J. C. M.; Koopal, L. K.; Bolt, G. H. *J. Colloid Interface Sci.* **1987**, *116*, 511.
- Zachara, J. M.; Girvin, D. C.; Schmidt, R. L.; Resch, C. T. *Environ. Sci. Technol.* **1987**, *21*, 589.
- Hayes, K. M.; Leckie, J. O. *J. Colloid Interface Sci.* **1987**, *115*, 564.
- Cowan, C. E.; Zachara, J. M.; Resch, C. T., in preparation.
- Hayes, K. M.; Roe, A. L.; Brown, G. E., Jr.; Hodgson, K. O.; Leckie, J. O.; Parks, G. A. *Science* **1987**, *238*, 783.
- Westall, J. *FITEQL, A Computer Program for Determination of Equilibrium Constants from Experimental Data Version 2.0*; 82-02; Department of Chemistry, Oregon State University: Corvallis, OR, 1982.
- Stroes-Gascoyne, S.; Kramer, J. R.; Snodgrass, W. J. *Environ. Sci. Technol.* **1986**, *20*, 1047.
- Schindler, P. W.; Fürst, B.; Dick, R.; Wolf, P. U. *J. Colloid Interface Sci.* **1976**, *55*, 469.
- Baes, C. F., Jr.; Mesmer, R. E. *Am. J. Sci.* **1981**, *281*, 935.
- Brown, P. L.; Sylva, R. N.; Ellis, J. J. *J. Chem. Soc., Dalton Trans.* **1985**, 723.
- Hunter, K. A.; Hawke, D. J.; Choo, L. K. *Geochim. Cosmochim. Acta* **1988**, *52*, 627.
- Baes, C. F., Jr.; Mesmer, R. E. *The Hydrolysis of Cations*; John Wiley and Sons, Inc.: New York, 1976; p 489.
- Hingston, F. J.; Posner, A. M.; Quirk, J. P. In *Adsorption from Aqueous Solution; Advances in Chemistry 79*; Gould, R. J., Ed.; American Chemical Society: Washington, DC, 1968; p 82.
- Yates, D. E. Ph.D. Dissertation, University of Melbourne, Melbourne, Victoria, Australia, 1975.
- Hsi, C.; Langmuir, D. *Geochim. Cosmochim. Acta* **1985**, *49*, 1931.
- Sanchez, A. L.; Murray, J. W.; Sibley, T. H. *Geochim. Cosmochim. Acta* **1985**, *49*, 2297.
- Dempsey, B. A.; Singer, P. C. In *Contaminants and Sediments*; Baker, R. A., Ed.; Ann Arbor Science: Ann Arbor, MI, 1980; p 334.
- Girvin, D. C.; Ames, L. L.; Schwab, A. P.; McGarragh, J. E. *J. Colloid Interface Sci.*, in press.
- Wagman, D. D.; Evans, W. H.; Parker, V. B.; Schumm, R. H.; Halow, I.; Bailey, S. M.; Churney, K. L.; Nuttall, R. L. *J. Phys. Chem. Ref. Data* **1982**, *11*, Suppl. 2.

(46) Cowan, C. E. Ph.D. Dissertation, University of Washington, Seattle, WA, 1986.

Received for review August 10, 1989. Revised manuscript received July 19, 1990. Accepted October 10, 1990. This work was supported by the U.S. Environmental Protection Agency, Athens

Environmental Research Laboratory, under a Related Services Agreement with the U.S. Department of Energy under Contract DE-AC06-76RL0 1830, Interagency Agreement DW90059-01. However, this paper has not been subject to Agency review and therefore does not necessarily reflect the views of the Agency and no official endorsement should be inferred.

Determination of Nitrogen Dioxide in Ambient Air by Use of a Passive Sampling Technique and Triethanolamine as Absorbent

Dariusz Krochmal* and Ludwik Górski

Institute of Inorganic Chemistry and Technology, Technical University of Cracow, ul. Warszawska 24, PL-31-155 Cracow, Poland

■ The effects of temperature, humidity, and storage on a diffusive sampler were tested by use of the Amaya-Sugiura method, modified previously. Several materials were used as carriers for triethanolamine in the sampler. The mass of NO₂ absorbed in the sampler was determined spectrophotometrically as nitrite by using Saltzman solution. The collection efficiency of the sampler was lower than that calculated from Fick's law of diffusion due to significant contribution of liquid phase in the overall sampler diffusive resistance. This resulted in an increase of the mass of NO₂ absorbed in the sampler by ca. 20% per 10 °C of temperature growth and by ca. 25% when the relative humidity rose from 0 to 100%. Dependence of concentration of TEA solution in the sampler on the relative humidity of the air was noted. The relative precision of the method characterized by RSD was 10%; the detection limit of NO₂ was 10 µg/m³ for a 24-h exposure.

Introduction

Since Levaggi et al. (1) applied triethanolamine (TEA) for the quantitative trapping of NO₂ from the air stream, this substance has frequently been used as an absorbent in passive sampling methods of determination of NO₂ (2-7). Our earlier studies (8) on the Amaya-Sugiura method (5) showed that parameters such as wind velocity and air temperature can seriously affect the accuracy of the method. While the face velocity effect was diminished to ~20% by an appropriate change in the sampler design (9), the temperature effect remained unchanged in spite of modification of the method. In this work an effort was made to measure and explain the temperature and humidity effects as due to the application of TEA as the absorbent.

As regards the modified sampler, it enables 24-h measurements of NO₂ concentrations in ambient air to be conducted at extremely low cost. The sampler is commercially available. The production cost of the sampler, which is reusable, is lower than 1 U.S. dollar. On the basis of the modified method, a Polish Standard (10) concerning determination of nitrogen dioxide in ambient air using a passive sampling technique was established this year.

Experimental Section

Analytical Procedure. The sampler design and analytical procedure were described elsewhere (9). A photograph of the sampler is presented in Figure 1. In some tests 25-mm disks of glass microfiber filters (Whatman GF/C), cellulose filters (Whatman 3), and different sorts of fiber materials produced by Śląskie Zakłady Przemysłu Lniarskiego "Lentex", Lubliniec, Poland (Catalog No.

46031 viscose fiber; Nos. 46012 and 46015 viscose polyester fiber) were used instead of nylon textile disks as triethanolamine (TEA) carriers.

Before relative humidity controlled tests, the samplers were prepared following the usual procedure and then kept open together with blanks for 24 h in a desiccator containing a constant-humidity atmosphere (see below).

Generation of Constant-Humidity Atmospheres.

The following saturated, aqueous solutions of inorganic substances were placed inside desiccators at 20 °C to obtain the relative humidity given in parentheses (11): H₃PO₄·1/2H₂O (9%), CaCl₂·6H₂O (32%), Ca(NO₃)₂·2H₂O (53%), NH₄Cl + KNO₃ (73%), NH₄Cl (79%), ZnSO₄·7H₂O (90%). For 0% RH, 5-Å molecular sieves were applied.

To evaluate the equilibrium curve between relative humidity and concentration of TEA, a series of measurements was carried out. For each value of relative humidity five samplers without caps were weighed to an accuracy of 1 mg; three of them were treated in the usual way with 0.1 mL of 20% (m/m) aqueous TEA solution, weighted again, and placed inside an appropriate desiccator at 20 °C together with the remaining two samplers. After 24 and 72 h, the samplers were weighed again. The final concentration of TEA was calculated after subtracting the average mass of humidity absorbed by the samplers that had not been treated with TEA.

Generation of Standard NO₂ Text Mixtures. Known concentrations of nitrogen dioxide were generated dynamically by using permeation devices. The system is shown schematically in Figure 2. A cleaned and dried air stream was pumped with a constant flow rate of 30 mL/min over a permeation device. The permeation device was held at 35 ± 0.1 °C in a thermostat. Several different permeation devices of the permeation rate (determined gravimetrically) of nitrogen dioxide ranging from 0.2 to 0.5 µg/min were applied. An additional permeation device containing sulfur dioxide (permeation rate 1.2 µg/min) was used for studies on interference effects. The total amount of NO₂ produced by a permeation device was diluted with another stream of purified air, whose flow rate was kept constant in the range of 5-10 L/min, depending on the desired NO₂ concentration. In relative humidity controlled experiments the diluting air was passed through a bubbler containing a constant-humidity solution (see above) to obtain a desired relative humidity. When the air was passed through a bubbler filled with distilled water, 100% RH (at a given temperature) was obtained. In the runs where the relative humidity was to be 0%, the air stream was additionally dried with 5-Å molecular sieves. The zero air was passed through a container where three samplers were exposed in each run. These samplers were then used